Chinese Chemical Letters 37 (2026) 111494

Contents lists available at ScienceDirect

Chinese Chemical Letters

journal homepage: www.elsevier.com/locate/cclet

g-C_3N_4/ZnO nano-reinforced polysulfonate-PVA dual-network hydrogels for enhanced antibacterial ability and breathable wound healing

Zhenyu Liu[b,1], Hizbullah Malik[e,1], Muhammad Bilal Khan Niazi[c,d,*], Umer Shahzad Malik[e], Zaib Jahan[f], Muhammad Salman Haider[e], Suhaib Umer Ilyas[g], Rayed S. Alshareef[h], Honghao Hou[b,*], Dong Yang[a,*]

[a] *Bioinspired Engineering and Biomechanics Center (BEBC), Key Laboratory of Biomedical Information Engineering of the Ministry of Education, School of Life Science and Technology, Xi'an Jiaotong University, Xi'an 710049, China*
[b] *School of Basic Medical Sciences, Guangdong Provincial Key Laboratory of Construction and Detection in Tissue Engineering, Southern Medical University, Guangzhou 510515, China*
[c] *Department of Chemical Engineering, King Fahd University of Petroleum and Minerals (KFUPM), Dhahran 31261, Kingdom of Saudi Arabia*
[d] *Interdisciplinary Research Center for Refining and Advanced Chemicals, King Fahd University of Petroleum and Minerals (KFUPM), Dhahran 31261, Kingdom of Saudi Arabia*
[e] *Department of Chemical Engineering, School of Chemical and Materials Engineering, National University of Science and Technology, Islamabad 44000, Pakistan*
[f] *Department of Mechanical Engineering, College of Engineering, Prince Mohammad Bin Fahd University, Al Khobar 31952, Kingdom of Saudi Arabia*
[g] *Chemical Engineering Department, University of Jeddah, Jeddah 23890, Kingdom of Saudi Arabia*
[h] *Chemical Engineering Department, College of Engineering, Taibah University Yanbu Al Bahr, 41911, Kingdom of Saudi Arabia*

ARTICLE INFO

Article history:
Received 13 March 2025
Revised 17 June 2025
Accepted 18 June 2025
Available online 18 June 2025

Keywords:
Wound healing
ZnO NPs
Membrane
Antibacterial activity
Breathability

ABSTRACT

Wound healing remains a significant challenge in medical science due to the complexity of the process. Hydrogels have emerged as promising materials for wound management, yet achieving non-cytotoxicity, biodegradability, and mechanical robustness in a single formulation continues to be a research focus. This study aims to develop polysulfonate-polyvinyl alcohol (PVA)/poly(2-acrylamido-2-methyl-1-propanesulfonic acid) (PAMPs) membranes reinforced with ZnO nanoparticles (NPs) and g-C_3N_4 to meet these requirements. The fabricated membranes were characterized using scanning electron microscopy (SEM), Fourier transform infrared spectroscopy (FTIR), X-ray diffraction (XRD), and atomic force microscopy (AFM), and were subjected to various biological evaluations including swelling ratios, water vapor transmission rates (WVTR), antibacterial activity, cytotoxicity, and *in-vivo* wound healing in a mouse model. The membranes exhibited mechanical strengths of 42.6 MPa and strains up to 183.35 %. XRD and FTIR confirmed the successful incorporation of ZnO NPs and g-C_3N_4, while SEM and AFM revealed a rough surface morphology conducive to cell adhesion. The membranes achieved moisture retention rates over 90 %, WVTR values up to 71.66 h g^{-1} m^{-2}, and swelling ratios as high as 116.06 %. Cytotoxicity tests demonstrated cellular viability exceeding 84.37 %, and antibacterial assays showed significant inhibition zones. *In vivo* studies indicated an 88.26 % wound healing rate within 9 days, surpassing traditional dressings and saline treatments. These results suggest that PAMPs/PVA/g-C_3N_4/ZnO membranes are found to be highly effective for wound dressing applications, combining superior mechanical properties, biocompatibility, and enhanced healing efficacy.

© 2026 Published by Elsevier B.V. on behalf of Chinese Chemical Society and Institute of Materia Medica, Chinese Academy of Medical Sciences.

Wound care poses significant challenges in healthcare, often exacerbated by infections, pain, and delayed healing, which can greatly impact patient recovery [1,2]. Skin injuries compromise the skin's barrier function, potentially leading to larger wound areas and higher mortality risks [3,4]. The cornerstone of effective wound management lies in advanced dressings [5], which should ideally protect against pathogens, maintain a favorable healing environment, and minimize complications [6–8]. Recent studies highlight the importance of maintaining moist wound conditions, in-

* Corresponding authors.
E-mail addresses: muhammad.niazi@kfupm.edu.sa (M.B.K. Niazi), ss.hhh89@hotmail.com (H. Hou), wsyangdong@gmail.com (D. Yang).
[1] These authors contributed equally to this work.

https://doi.org/10.1016/j.cclet.2025.111494
1001-8417/© 2026 Published by Elsevier B.V. on behalf of Chinese Chemical Society and Institute of Materia Medica, Chinese Academy of Medical Sciences.

creasing the demand for dressings that promote gas exchange, manage exudate, and have antimicrobial properties [9,10].

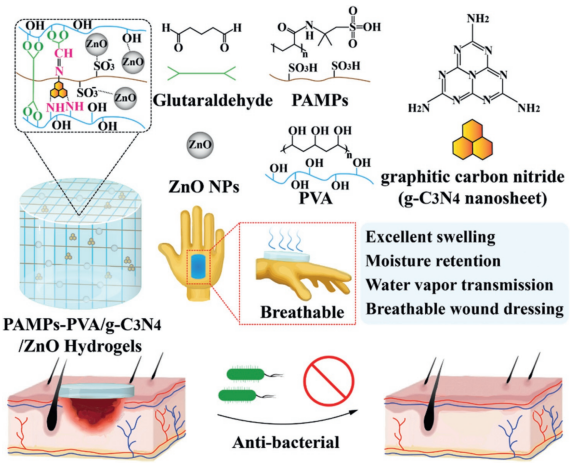
Chronic infected wounds continue to be a major health issue worldwide, as bacterial colonization worsens tissue damage and symptoms [11–13]. Nanocomposite hydrogels are promising options because their three-dimensional polymer networks can hold large amounts of water without breaking down, helping to keep the wound moist and promote healing [14–16]. They are highly compatible with biological tissues, mimicking the natural extracellular matrix, and can be adjusted to have specific biochemical and mechanical properties [17–19]. This makes them useful for various applications, including wound care, biosensors, and antibacterial coatings [20–22].

Polyvinyl alcohol (PVA) is a common synthetic biopolymer that provides flexibility to fit around tissues, allows gases to pass through to prevent the growth of anaerobic bacteria, and is compatible with living tissues [23–26]. However, its natural stiffness limits some uses in medicine, so it is often mixed with materials like chitosan, hyaluronic acid, or alginate to make it more flexible [27,28]. New materials such as poly(2-acrylamido-2-methyl-1-propanesulfonic acid) (PAMPs) can mimic natural substances like heparin and taurine, offering good water affinity, sensitivity to pH, antimicrobial effects, and low toxicity [29].

Adding nanoparticles (NPs) can improve the properties of hydrogels even more. Zinc oxide (ZnO) NPs are recognized as safe by the Food and Drug Administration (21CFR182.8991) and provide antimicrobial, anticancer, and antioxidant benefits that are compatible with tissues [30]. Graphitic carbon nitride (g-C_3N_4) helps strengthen the hydrogel mechanically thanks to its high heat stability, electrical conductivity, and large surface area. It also supports antibacterial light therapy and fluorescence imaging. During production, careful control of the structure is important to keep these features stable and effective [31–33].

In this study, nanocomposite hydrogel membranes were fabricated by incorporating g-C_3N_4 nanosheets and ZnO NPs into PAMPs-PVA networks. While PAMPs are known to balance rigidity and elasticity in PVA matrices, the synergistic effects of g-C_3N_4 and ZnO NPs in enhancing antibacterial activity, mechanical strength, and wound healing efficacy remain underexplored. The integration of g-C_3N_4 aims to leverage its photocatalytic antibacterial properties and improve surface roughness, whereas the incorporation of ZnO NPs is intended to exploit their broad-spectrum antibacterial activity and biocompatibility. Additionally, the potential of sulfonic pendant groups in PAMPs to mimic glycosaminoglycan molecules for enhanced healing has yet to be fully investigated in the context of hydrogel dressings (Scheme 1). The novel integration of these polymers and advanced NPs presents a promising alternative to conventional wound dressings, which often lack the dual functionality of elasticity and antimicrobial properties. This approach could potentially replace existing technologies by providing superior healing environments and infection control. The significant focus of this research lies in optimizing the mechanical and biological properties of the hydrogel membranes, particularly targeting their antimicrobial efficacy and wound-healing promotion in chronic and acute wound management.

Fourier transform infrared (FTIR) spectroscopy characterized functional groups and crosslinking reactions in the fabricated films (Fig. S1a in Supporting information). A broad peak at 3500 cm^{-1} aligns with the O–H stretching vibrations from both PVA and PAMPS. The peak at 3000 cm^{-1} is attributed to the asymmetric stretching of C–H groups in the methylene units of PVA. Peaks at 1645, 1550, and 1128 cm^{-1} are assigned to the C=O stretching, N–H bending, and S-O stretching of the sulfonic acid groups, respectively. Critically, the peak at 1095 cm^{-1} confirmed C–O-C formation, evidencing crosslinking between PVA and glutaraldehyde [11]. Incorporation of g-C_3N_4 in PPZC0 induced slight peak shifts



Scheme 1. Schematic synthetic process of PAMPs/PVA/g-C_3N_4/ZnO nanocomposite hydrogel membrane, which exhibits excellent air permeability and antimicrobial activity potential, and can be used for wound healing.

and generated a distinct 806 cm^{-1} peak corresponding to triazine unit breathing modes, verifying g-C_3N_4 integration. For PPZC150 (PAMPS-PVA/g-C_3N_4/ZnO), a minor peak at 450–480 cm^{-1} indicated Zn-O stretching vibrations [34], confirming successful ZnO NP incorporation.

X-ray diffraction (XRD) analysis elucidated the crystalline structure of the fabricated membrane. As depicted in Fig. S1b (Supporting information), the peak at approximately 19.27° is associated with the semi-crystalline plane of PVA, indicating the formation of intermolecular hydrogen bonds within the hydrogel [3]. A weak peak observed at 27.6° corresponds to the interlayer stacking of conjugated aromatic planes in g-C_3N_4 [11]. The addition of NPs increased the crystallinity of the fabricated membranes, as evidenced by the peaks at 31.83°, 34.55°, 36.37°, 47.75°, and 56.74°, indicating the presence of ZnO NPs [35]. The presence of these characteristic peaks within the polymeric matrix confirms the successful fabrication of the composite membranes and highlights the excellent compatibility of the PAMPs-PVA membrane with g-C_3N_4 nanosheets and ZnO NPs.

The surface morphology of the fabricated PAMPs-PVA membranes, reinforced with g-C_3N_4 and ZnO NPs, was assessed using scanning electron microscopy (SEM). The SEM images, presented in Fig. S2 (Supporting information), reveal a dense and compact morphology with no visible pores. The surface of the PAMPs-PVA membrane appears homogeneous and smooth, indicating effective cross-linking by glutaraldehyde (GA) within the polymeric network. The incorporation of g-C_3N_4 introduced slight surface roughness to the PAMPs-PVA membrane, as evidenced by the presence of small footprints in the SEM images. Similar observations were reported by Malik *et al.* [3]. Whereas, the incorporation of ZnO NPs resulted in a smoother surface compared to the PAMPs-PVA/g-C_3N_4 membrane, suggesting excellent dispersion of the NPs. However, some localized agglomerations of NPs suggest incomplete mixing of the metallic NPs. This increase in surface roughness is advantageous, as it contributes to expanding the specific surface area.This increase in roughness is beneficial as it helps expand the specific surface area [36]. This minor heterogeneity is not detrimental to biomedical applications, where mechanical stability is often more critical than the complete solubility of NPs.

The surface topography of the fabricated membranes was examined using atomic force microscopy (AFM). The AFM images presented in Fig. S3 (Supporting information). The PAMPs-PVA and PAMPs-PVA/g-C_3N_4 membranes exhibited root mean square (RMS) surface roughness values of 863.8 and 986.1 pm, and heights

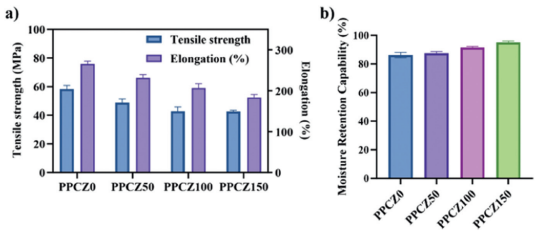


Fig. 1. (a) The mechanical strength and (b) moisture retention capability of the fabricated membranes. Data are presented as mean ± standard deviation (SD) ($n = 3$).

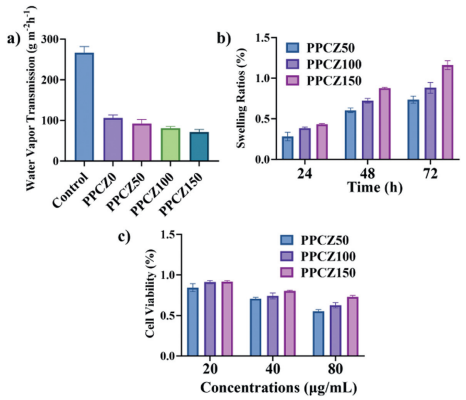


Fig. 2. (a) The water vapor transmission, (b) swelling ratios, and (c) cell viability of the fabricated membranes. Data are presented as mean ± SD ($n = 3$).

of 9.1 and 10 nm, respectively. The AFM analysis of the PAMPs-PVA/g-C_3N_4/ZnO membrane, which exhibits an RMS roughness of 2.817 nm and a height of 25.8 nm. The increased surface roughness with the addition of NPs corroborates the SEM results which indicates that incorporating of NPs significantly enhances surface roughness. In medical applications, this increased surface roughness is beneficial as it improves cell adhesion, proliferation, and interaction [37,38].

Subsequent experiments were conducted using four concentration gradients (Table S1 in Supporting information) to systematically investigate the critical role of ZnO NP concentrations in balancing antibacterial activity, mechanical strength, and biocompatibility of the fabricated membranes. The stress-strain graph of the fabricated membranes is shown in Fig. 1a. The stress values for the PPCZ0, PPCZ50, PPCZ100, and PPCZ150 membranes were found to be 58.35 ± 2.07, 48.79 ± 2.16, 42.83 ± 2.45, and 42.6 ± 0.69 MPa, respectively. The Young's modulus values were calculated using the slope of the linear region in the stress-strain graph. Corresponding strain values were 265.13 %, 231.42 %, 206.54 %, and 183.35 %. The results indicate that the mechanical strength decreased with the addition of NPs. Similar findings have been reported by other authors, who observed that incorporating NPs decreased the mechanical strength of membranes [11,39]. This reduction in strength may be attributed to the fact that the extended flow of the polymer chains reduces the plasticity of the membranes, making them more brittle. Crucially, all formulations exceeded human skin's breaking stress threshold (35 MPa) [40], confirming their clinical adequacy for wound dressing applications despite strength reduction trends.

The moisture retention ability of hydrogel membranes is a critical factor for wound dressing applications, as it determines how well the membrane can maintain moisture, regulate exudate adsorption, and interact with the wound. Hydrogels are known for their high-water content, which supports faster wound healing. The moisture retention properties of the membranes are illustrated in Fig. 1b. The results demonstrated retention rates of 86.19 % ± 1.60 %, 87.55 % ± 1.04 %, 91.58 % ± 0.58 % and 95.00 % ± 0.87 % for PAMS-PVA, PPCZ0, PPCZ50, PPCZ100, and PPCZ150, respectively. Although the moisture retention decreased slightly with increasing NP concentration, the reduction was minor. This consistent performance is attributed to the hydrophilic nature of both PVA and PAMPS, which readily form hydrogen bonds with water molecules [41]. Overall, the membranes exhibited excellent moisture retention properties, making them promising candidates for wound dressing materials.

The water vapor transmission rate (WVTR) determination test was conducted to evaluate the ability of the fabricated membranes to regulate water transmission, which is crucial for wound dressing applications (Fig. 2a). In this test, open and closed bottles served as sham and control, respectively. The WVTR for the positive control was 266.61 ± 12.53 h g^{-1} m^{-2}, which significantly decreased to 105.83 ± 6.25 h g^{-1} m^{-2} when tested with PAMPs-PVA/g-C_3N_4 membrane. For membranes containing ZnO NPs at concentrations of 50, 100, and 150 mg, the WVTR values were 92.00 ± 8.50, 80.94 ± 3.40, and 71.66 ± 5.17 h g^{-1} m^{-2}, respectively. This decreasing trend indicates that ZnO NPs effectively hinder water vapor transmission by acting as barriers within the PAMPs-PVA matrix, as confirmed by XRD and SEM analyses. The XRD results showed a reduction in the PVA peak intensity with increasing ZnO concentration, while SEM images revealed increased compaction of the membranes with higher NP content. According to Ahmed *et al.* [41], an effective WVTR for wound healing should be below 120 h g^{-1} m^{-2}. All tested membranes fell within this optimal range, demonstrating that our synthesized membranes exhibit superior performance and are well-suited for advanced wound dressing applications.

The swelling abilities of the fabricated membranes were evaluated to determine their effectiveness in medical applications, particularly for absorbing exudates and preventing wound maceration, which promotes faster healing. The membranes were immersed in water for a total of 72 h, with swelling measurements taken at 24-h intervals. The results are illustrated in Fig. 2b. The initial swelling percentages were 28.20 %, 38.43 %, and 43.17 % for PPCZ50, PPCZ100, and PPCZ150, respectively. By the third day, they further increased to 73.49 %, 88.15 %, and 116.06 %, respectively. The hydroxyl and sulfonic acid groups of the hydrophilic polymer PVA/PAMPs lock in moisture through hydrogen bonding, giving the prepared membranes excellent moisturizing ability and providing the material with a high swelling ratio, allowing it to effectively absorb exudate. Meanwhile, the crosslinking density and the dense structure formed by NPs balance moisture retention and evaporation, maintaining a moist environment, as well as the hydrophilic nature of ZnO NPs, as reported by Hia *et al.* [30] and Sayyar *et al.* [35]. These results demonstrate that the fabricated membranes exhibit excellent swelling properties, making them highly suitable for biomedical applications, particularly wound management. Their ability to absorb substantial amounts of exudate ensures effective wound care and supports accelerated healing.

The MTT assay evaluated cell viability and metabolic activity of the membranes (Fig. 2c) for PPCZ0, PPCZ50, and PPCZ150, tested at concentrations ranging from 20 μg/mL to 80 μg/mL. After 24 h, phosphate-buffered saline (PBS) incubation and supernatant analysis, results revealed concentration-dependent viability: PPCZ0 declined from 73 % to 55.33 %, PPCZ50 from 80.16 % to 70.87 %, and PPCZ150 from 91 % to 84.37 %. As the concentration increased, cell viability decreased, and cytotoxicity increased, consistent with previous studies using similar compositions of polymers and NPs, such as those by Jiang *et al.* [42]. Notably, PPCZ150 showed good viability even at higher concentrations. This demonstrates excellent biocompatibility and non-toxicity, confirming the membranes' suitability for wound dressings and biomedical applications.

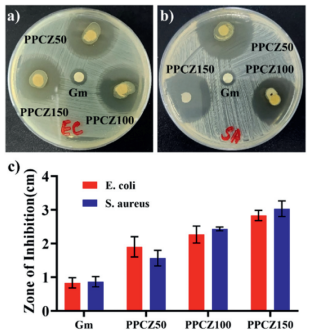


Fig. 3. Photographs depicting the zone of inhibition around PAMPs-PVA against (a) *S. aureus* and (b) *E. coli*. Additionally, (c) presents a graphical representation of the antibacterial activity of the membranes. Data are presented as mean ± SD ($n = 3$).

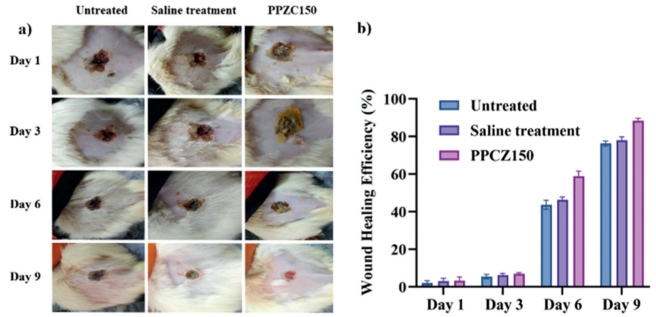


Fig. 4. (a) The wound healing treatment progression over several days and (b) graphical illustration representation of wound healing efficiency. Data are presented as mean ± SD ($n = 3$).

The antibacterial activity of the fabricated membranes was evaluated using the disc diffusion method against Gram-positive *Staphylococcus aureus* (*S. aureus*) and Gram-negative *Escherichia coli* (*E. coli*). This method revealed clear and substantial zones of inhibition around the membranes. As shown in Figs. 3a and b. The synthesized membranes exhibited enhanced antibacterial activity at higher NP concentrations, indicating effective antibacterial properties [43]. Notably, larger inhibition zones against Gram-positive *vs.* Gram-negative bacteria were observed, attributable to structural differences in cell walls [44]: Gram-positive bacteria possess thick peptidoglycan layers more susceptible to damage. As illustrated in Fig. 3c, Gentamicin was used as a positive control, producing inhibition zones of 0.82 ± 0.13 cm for *S. aureus* and 0.87 ± 0.12 cm for *E. coli*. Specifically, the inhibition zones for *E. coli* were 1.9 ± 0.24, 2.27 ± 0.21, and 2.83 ± 0.12 cm. For *S. aureus*, they were 1.57 ± 0.19, 2.43 ± 0.05, and 3.03 ± 0.19 cm for PPCZ50, PPCZ100, and PPCZ150. In contrast, Gram-negative bacteria exhibit complex outer membranes with reduced antimicrobial permeability. The observed NP concentration-dependent antibacterial efficacy aligns with Zhang *et al.* [45] and Jiang *et al.* [42], where larger inhibition zones against *S. aureus* vs. *E. coli* were consistently noted. Enhanced activity stems from ZnO NP release, generating ROS to damage cell walls, while Zn^{2+} ions penetrate membranes, releasing lipopolysaccharides to compromise structural integrity [33]. These mechanisms are modulated by membrane crystallinity, surface charge, and area [46]. Collectively, the membranes demonstrate potent bacterial inhibition, supporting their utility in wound dressings.

In the *in-vivo* wound healing experiment, secondary burns and wound incisions were performed on rats, with healing progress measured at intervals on days 1, 3, 6, and 9. All experimental animals were purchased from the Animal Center of Southern Medical University, and animal experiments were approved by the Animal Ethics Committee of Southern Medical University. The efficacy of the fabricated membranes was assessed by measuring the wound size at regular intervals and comparing it to the initial wound size. The results, depicted in Fig. 4, clearly show that the most effective results were observed with PAMPs-PVA/g-C_3N_4/ZnO membranes, which outperformed saline-treated wounds, demonstrating the superiority of the fabricated membranes. By day 9, the healing percentages increased to 76.27 % ± 1.13 %, 77.93 % ± 1.54 %, and 88.26 % ± 1.09 % for untreated, saline-treated, and PPCZ150 membrane-treated wounds, respectively, with membrane-treated wounds showing significantly higher healing rates. The wounds treated with the fabricated membranes healed significantly faster compared to untreated wounds, indicating that the membranes are highly effective for burn wound treatment. No postoperative infections were observed, further confirming the suitability of these membranes for wound care applications.

In conclusions, PAMPs/PVA hydrogel membranes enhanced with ZnO NPs and g-C_3N_4 were successfully fabricated. Structural characterization confirmed a rough surface morphology, while XRD/FTIR verified filler integration and hydrogen bond formation. The membranes exhibited optimal functional properties: high moisture retention, ideal WVTR, and significant swelling capacity—collectively maintaining a moist wound environment. Cytotoxicity tests demonstrated exceeded 91 % cell viability, and antibacterial assays revealed substantial inhibition zones. In vivo evaluation on rat burn models showed around 89 % wound closure within 9 days. These findings suggest that PAMPs/PVA/g-C_3N_4/ZnO membranes are highly effective for wound dressing applications, combining enhanced mechanical properties, biocompatibility, and antibacterial activity. These membranes provide a novel solution for advanced wound care through synergistic multifunctional mechanisms, particularly suitable for complex infected wounds, with the potential to reduce antibiotic reliance and shorten healing cycles. Future functional modifications could further enable personalized precision therapeutics.

Declaration of competing interest

The authors declare that they have no known competing financial interests or personal relationships that could have appeared to influence the work reported in this paper.

CRediT authorship contribution statement

Zhenyu Liu: Writing – review & editing, Writing – original draft, Methodology, Formal analysis, Data curation, Conceptualization. **Hizbullah Malik:** Writing – review & editing, Writing – original draft, Project administration, Methodology. **Muhammad Bilal Khan Niazi:** Writing – review & editing, Methodology, Investigation, Data curation, Conceptualization. **Umer Shahzad Malik:** Resources, Project administration, Methodology, Investigation. **Zaib Jahan:** Supervision, Resources, Project administration. **Muhammad Salman Haider:** Project administration, Investigation, Formal analysis. **Suhaib Umer Ilyas:** Software, Project administration, Investigation. **Rayed S. Alshareef:** Software, Project administration, Investigation. **Honghao Hou:** Writing – review & editing, Project administration, Funding acquisition, Conceptualization. **Dong Yang:** Software, Resources, Project administration.

Acknowledgments

This work was supported by the National Key R&D Program of China (No. 2023YFC2412800), National Natural Science Foundation of China (Nos. 32371410, 52003113), Guangdong Basic and Applied Basic Research Foundation (Nos. 2023B1515120055,

2024A1515011482), Key Program for Int. Cooperation of Shaanxi Province (No. 2023-GHZD-26), Scientific Research Staring Foundation for the Returned Overseas Chinese Scholars, Shaanxi Province (No. 71240000000002), and Science Foundation for Post Doctorate Research of Shanxi Province (No. 31271000000040).

Supplementary materials

Supplementary material associated with this article can be found, in the online version, at doi:10.1016/j.cclet.2025.111494.

References

[1] N. Zhang, X. Zhang, Y. Zhu, et al., Int. J. Biol. Macromol. 264 (2024) 130625.
[2] S.M. Hosseini, M. Abdouss, S. Mazinani, et al., Compos. Part B: Eng. 231 (2022) 109557.
[3] U.S. Malik, Q. Duan, M.B.K. Niazi, et al., Chin. Chem. Lett. 34 (2023) 108071.
[4] R.C. Op't Veld, X.F. Walboomers, J.A. Jansen, et al., Tissue Eng. Part. B: Rev. 26 (2020) 230–248.
[5] D. Li, Z. Liu, L. Zhang, et al., Nat. Commun. 15 (2024) 8637.
[6] D. Pranantyo, C.K. Yeo, Y. Wu, et al., Nat. Commun. 15 (2024) 954.
[7] A. du Halgouet, A. Darbois, M. Alkobtawi, et al., Immunity 56 (2023) 78-92.e76.
[8] W. Hu, X. Zhang, Z. Liu, et al., iScience 27 (2024) 109545.
[9] A. Zhang, G. Zhao, G. Xiang, et al., Chin. Chem. Lett. 36 (2025) 110767.
[10] C. Hu, C. Chu, L. Liu, et al., Sci. Adv. 7 (2021) eabf0787.
[11] C. Pu, R. Lin, S. Liang, et al., Trends Chem. 5 (2023) 88–101.
[12] M. Zhang, F. Deng, L. Tang, et al., Chem. Eng. J. 405 (2021) 126756.
[13] U.S. Malik, M.B.K. Niazi, Z. Jahan, et al., Environ. Chem. Lett. 20 (2022) 495–517.
[14] S. Liu, J. Zhan, Z. Liu, et al., Carbohyd. Polymers 352 (2025) 123192.
[15] Y. Fu, Z. Li, S. Zhao, et al., Sci. Adv. 10 (2024) eadk4080.
[16] S. Liu, J.M. Yu, Y.C. Gan, et al., Milit. Med. Res. 10 (2023) 16.
[17] X. Song, J. Zhang, S. Shen, et al., Research 6 (2023) 0161.
[18] Y. Hu, J. Zhan, C. Pu, et al., Chem. Eng. J. 509 (2025) 161269.
[19] J. Wang, Z. Gao, H. Liang, et al., Chin. Chem. Lett. 36 (2025) 110569.
[20] R. Song, H. Xie, G. Liu, Chin. Chem. Lett. 36 (2025) 110442.
[21] P. Patil, K.A. Russo, J.T. McCune, et al., Sci. Translat. Med. 14 (2022) eabm6586.
[22] E. Shirzaei Sani, C. Xu, C. Wang, et al., Sci. Adv. 9 (2023) eadf7388.
[23] L. Serairi, C. Santillo, P. Basset, et al., Adv. Mater. 36 (2024) 2403366.
[24] X. Liu, X. Qiu, L. Nie, et al., ACS Nano 18 (2024) 17651–17671.
[25] G. Hong, J. Li, W. Wei, et al., ACS Nano 19 (2025) 10180–10198.
[26] R. Niranjan, M. Kaushik, J. Prakash, et al., Inorg. Chem. Commun. 154 (2023) 110885.
[27] E.A. Kamoun, E.R.S. Kenawy, T.M. Tamer, et al., Arab. J. Chem. 8 (2015) 38–47.
[28] L.C. Lee, K.T. Huang, Y.T. Lin, et al., Small 20 (2024) 2311811.
[29] Y. Cheng, T. Zhu, Q. He, et al., Adv. Funct. Mater. 35 (2025) 2500186.
[30] E.M. Hia, S.R. Jang, B. Maharjan, et al., Colloids Surf. B: Biointerfaces 236 (2024) 113804.
[31] X. Xu, X. Zhang, H. He, et al., Langmuir 40 (2024) 15389–15406.
[32] A. Alaghmandfard, K. Ghandi, Nanomaterials 12 (2022) 294.
[33] O. Iqbal, H. Ali, N. Li, et al., Mater. Today Phys. 34 (2023) 101080.
[34] K. Thakur, A. Rajhans, B. Kandasubramanian, Environ. Sci. Pollut. Res. Int. 26 (2019) 32013–32028.
[35] Z. Sayyar, Z. Hosseini, P. Mohammadzadeh Pakdel, A. Hassani, J. Water Process Eng. 63 (2024) 105449.
[36] D.B. Ji, J.L. Yang, T.Y. Wang, et al., Separat. Purif. Technol. 338 (2024) 126568.
[37] Y. Hou, L. Yu, W. Xie, et al., Nano Lett. 20 (2020) 748–757.
[38] K. Devi, A. Sharma, R. Kumar, B. Singh, Med. Novel Technol. Devices 22 (2024) 100303.
[39] L. Yang, L. Ren, Y. Zhao, et al., Int. J. Biol. Macromol. 226 (2023) 184–193.
[40] C. Amante, T. Esposito, P. Del Gaudio, et al., Majumdar 20 (2006) 59–67.
[41] A. Ahmed, M.B.K. Niazi, Z. Jahan, et al., Eur. Polymer J. 130 (2020) 109650.
[42] L. Jiang, B. Jiang, J. Xu, T. Wang, Int. J. Biol. Macromol. 253 (2023) 126628.
[43] L. Jiang, Y. Han, J. Xu, T. Wang, Biochem. Eng. J. 184 (2022) 108488.
[44] M. Zhai, Y. Xu, B. Zhou, W. Jing, J. Photochem. Photobiol. B: Biol. 180 (2018) 253–258.
[45] X. Zhang, Q. Liu, S. Zhu, M. Yu, Materials Today Commun 33 (2022) 104355.
[46] S. Baghaie, M.T. Khorasani, A. Zarrabi, J. Moshtaghian, J. Biomater. Sci. Polymer Ed. 28 (2017) 2220–2241.